Weierstraß-Institut

für Angewandte Analysis und Stochastik

Leibniz-Institut im Forschungsverbund Berlin e. V.

Preprint ISSN 2198-5855

On the grad-div stabilization for the steady Oseen and Navier-Stokes equations

Naveed Ahmed[1]

submitted: December 8, 2015

[1] Weierstrass Institute
Mohrenstr. 39
10117 Berlin
Germany
email: Naveed.Ahmed@wias-berlin.de

No. 2188

Berlin 2015

2010 *Mathematics Subject Classification.* 35Q30, 76M10, 65L60.

Key words and phrases. incompressible Navier–Stokes equations, mixed fnite elements, grad-div stabilization, error estimates, stabilization parameter.

Edited by
Weierstraß-Institut für Angewandte Analysis und Stochastik (WIAS)
Leibniz-Institut im Forschungsverbund Berlin e. V.
Mohrenstraße 39
10117 Berlin
Germany

Fax: +49 30 20372-303
E-Mail: preprint@wias-berlin.de
World Wide Web: http://www.wias-berlin.de/

Abstract

This paper studies the parameter choice in the grad-div stabilization applied to the generalized problems of Oseen type. Stabilization parameters based on minimizing the $H^1(\Omega)$ error of the velocity are derived which do not depend on the viscosity parameter. For the proposed parameter choices, the $H^1(\Omega)$ error of the velocity is derived that shows a direct dependence on the viscosity parameter. Differences and common features to the situation for the Stokes equations are discussed. Numerical studies are presented which confirm the theoretical results. Moreover, for the Navier-Stokes equations, numerical simulations were performed on a two-dimensional flow past a circular cylinder. It turns out, for the MINI element, that the best results can be obtained without grad-div stabilization.

1. Introduction

Incompressible flows are modeled by the incompressible Navier-Stokes equations which are given by

$$\left\{\begin{array}{rcll} -\nu\Delta\mathbf{u}+\mathbf{u}\cdot\nabla\mathbf{u}+\nabla p &=& \mathbf{f} & \text{in } \Omega, \\ \nabla\cdot\mathbf{u} &=& 0 & \text{in } \Omega, \\ \mathbf{u} &=& \mathbf{0} & \text{on } \Gamma, \end{array}\right. \tag{1}$$

where $\mathbf{f}$ models body forces acting on the flow and ν is the inverse of the Reynolds number. In the high Reynolds number flow problems, one typically observe that $\nu \ll 1$. Hence, a stabilization of the Galerkin finite element formulation is necessary. A popular remedy is to add a term based on the streamline upwind Petrov-Galerkin (SUPG) [1] to the finite element formulation that accounts for stabilizing dominating convection. However, a main difficulty in the analysis of the SUPG method comes from the coupling between velocity and pressure term. It is suggested in [2, 3] that an additional stabilization, the so called grad-div stabilization, is important for the robustness. In [4], a combination of the SUPG and grad-div stabilization methods were studied for the generalized Oseen equations. It was concluded that the SUPG method is less important for the inf-sup stable pair of velocity and pressure due to the constant in the stabilization parameter which depended on the problem data. The authors also showed that the numerical instabilities occur for slightly distorted quasi-uniform meshes. Furthermore, considering only the grad-div stabilization, it is acknowledged that the grad-div stabilization is more important and leads to satisfactory results.

The grad-div stabilization has been used as a successful approach to improve the mass conservation and reduces the velocity error caused by the pressure error in the simulations of incompressible flow problems. In the finite element formulation, the grad-div term which is based on the residual of the continuity equation adds the stabilizing term $\gamma(\nabla\cdot\mathbf{u}_h, \nabla\cdot\mathbf{v}_h)$ to the momentum equation.

Such a term also occurs in the subgrid pressure model in the framework of scales separation of variational multiscale formulation of Navier-Stokes equations [5, 6]. Numerical studies presented in [7] also shows that the grad-div stabilization is useful for practical use of some turbulence models.

The primary objective of this paper is to study the choice of optimal parameter for grad-div stabilization in mixed finite element methods for the Oseen and Navier-Stokes equations (1).

Theoretical analysis and numerical simulations performed for the inf-sup stable pair of element, see e.g., [8, 9, 10], indicate that $\gamma = \mathcal{O}(1)$ is often a good choice. Further, considering only the grad-div stabilization in [4], it is demonstrated that the optimal parameter should be chosen to $\gamma = 10^{-1}$. A theoretical analysis proposed in [11] also suggests that the stabilization parameter should be $\mathcal{O}(1)$ for the inf-sup stable elements. However, in [12] it was shown that in certain situations, an optimal γ can be much larger than $\mathcal{O}(1)$, depending on the size of pressure relative to the size of the velocity. Furthermore, for solutions with large or complicated pressures, good results were obtained with $\gamma = 10^4$ and bad results with $\gamma = 1$ or 10.

A detailed investigation of the optimal grad-div stabilization parameter γ in mixed finite element methods for the Stokes equation can be found in [13]. Optimal parameters are derived using the H^1-norm of the velocity error and L^2-norm of the pressure. Based on minimizing the H^1-norm of velocity error, it was shown that the optimal parameter depends on the magnitude of the pressure relative to the velocity in the appropriate norms. However, it is independent of the viscosity and pressure if an appropriate stabilization parameter is used and a pointwise divergence-free subspace with optimal approximation space exists. Moreover, it was shown that a good choice of stabilization parameters for minimizing the $H^1(\Omega)$ velocity error compared to the L^2 error of the pressure gives larger parameters.

The main contribution of this manuscript is the extension of the idea presented for the Stokes problem in [13] to the Oseen equations which can be viewed as a direct linearization (fixed point iteration) of the steady state or time dependent Navier-Stokes equations. The pointwise divergence-free velocity spaces will be used that eliminate the effect of pressure on the velocity error, and which relies on special grids and optimal approximation properties of the subspace. For the sake of brevity, the minimization of $H^1(\Omega)$ error of velocity will be taken into account for finding the optimal parameter in the grad-div stabilization.

Compared to the Stokes problem considered in [13], the main observations for the Oseen problem are:

- For the Taylor-Hood element on the barycentric refined grids and MINI element on the union-jack triangulations, the optimal parameter γ is independent of the viscosity parameter ν. In contrast an increase in the parameter γ was predicted when decreasing ν in the Stokes problem. This holds for the case when the divergence-free subspace of the velocity space has optimal approximation properties. Another finding in comparison to the Stokes problem is that the decrease in ν leads to smaller values of optimal γ for both elements. Furthermore, for the MINI element, the optimal parameter γ decreases with mesh width h but this is not true for the Taylor-Hood element.

- If the divergence-free subspace of velocity space does not have the optimal approximation properties, the optimal γ behave more or less similar as in the Stokes problem.

- Irrespective of the optimal approximation properties of the divergence-free subspace of the velocity space, it is observed by inserting the proposed stabilization parameter γ into the error estimates leads to the error bound that depends on the ν. Hence, the error bound increases by decreasing ν.

Numerical simulations for the steady-state flow around a circular cylinder suggests for the MINI element on standard as well as on Delauney type grids that the grad-div stabilization is not useful to improve the accuracy of the computed solution for such type of elements. Furthermore, the use of inf-sup stable Taylor-Hood finite element with optimal parameter leads to accurate results when compared to the reference data [14].

The remainder of the paper is organized as follows: Section 2 introduces the notations and finite element discretization of the Oseen problem. In Section 3, error estimates based on minimizing the H^1 norm of the velocity are presented which leads to the good parameter choices of the

stabilization parameter γ for different approximation properties of the pointwise divergence-free subspace. Section 4 gives some numerical tests which supports the theoretical results. It is shown that, depending on the finite element spaces and the mesh, the optimal parameter vary from $\mathcal{O}(h^2)$ to $\mathcal{O}(10^4)$. A similar observation can be found in [13]. The paper concludes with a summary of the results.

2. A linearized Navier-Stokes problem

Consider an auxiliary problem of generalized Oseen type:

$$\left\{\begin{array}{rcll} -\nu\Delta\mathbf{u} + \mathbf{b}\cdot\nabla\mathbf{u} + \sigma\mathbf{u} + \nabla p &=& \mathbf{f} & \text{in } \Omega, \\ \nabla\cdot\mathbf{u} &=& 0 & \text{in } \Omega, \\ \mathbf{u} &=& \mathbf{0} & \text{on } \Gamma. \end{array}\right. \tag{2}$$

This equation can be viewed as (a fixed point) a linearization of the steady-state Navier-Stoke problem (1) with $\sigma = 0$. Here, $\Omega \subset \mathbb{R}^d$ $d = \{2, 3\}$ be a bounded domain, $\mathbf{u}$ the velocity, p the pressure, $\mathbf{f}$ a given source term and ν the kinematic viscosity. To simplify the presentation, we restrict ourselves to the cases $\sigma = 0$ and $\sigma = 1$.

Throughout this paper, the standard notations for Lebesgue and Sobolev spaces will be used. The L^2 inner product in a domain Ω is denoted by $(\cdot,\cdot)$ and the corresponding norm by $\|\cdot\|_0$.

Throughout this paper, the standard notations for Lebesgue and Sobolev spaces will be used. The L^2 inner product in a domain Ω is denoted by $(\cdot,\cdot)$ and the corresponding norm by $\|\cdot\|_0$.

Consider the function spaces for velocity and pressure $V := H_0^1(\Omega)^d$ and $Q := L_0^2(\Omega)$, respectively, the variational formulation of (2) reads:

Find $(\mathbf{u}, p) \in V \times Q$ such that for all $(\mathbf{u}, p) \in H_0^1(\Omega)^d \times L_0^2(\Omega)$ it holds

$$\left\{\begin{array}{rcl} \nu(\nabla\mathbf{u}, \nabla\mathbf{v}) + b_s(\mathbf{b}; \mathbf{u}, \mathbf{v}) + \sigma(\mathbf{u}, \mathbf{v}) - (\nabla\cdot\mathbf{v}, p) &=& (\mathbf{f}, \mathbf{v}), \\ (\nabla\cdot\mathbf{u}, q) &=& 0 \end{array}\right. \tag{3}$$

Let the finite element discretization of (3) with the pairs of conforming finite element spaces $V_h \subset V$ and $Q_h \subset Q$ that satisfies the inf-sup compatibility condition

$$\inf_{q_h \in Q_h} \sup_{\mathbf{v}_h \in V_h} \frac{(\nabla\cdot\mathbf{v}_h, q_h)}{\|\nabla\mathbf{v}_h\|_0 \|q_h\|_0} \geq \beta > 0. \tag{4}$$

The finite element formulation of (3) reads:

Find $(\mathbf{u}_h, p_h) \in V_h \times Q_h$ such that for all $(\mathbf{v}_h, q_h) \in V_h \times Q_h$

$$\left\{\begin{array}{rcl} \nu(\nabla\mathbf{u}_h, \nabla\mathbf{v}_h) + b_s(\mathbf{b}; \mathbf{u}_h, \mathbf{v}_h) + \sigma(\mathbf{u}_h, \mathbf{v}_h) + \gamma(\nabla\cdot\mathbf{u}_h, \nabla\mathbf{v}_h) - (\nabla\cdot\mathbf{v}_h, p_h) &=& (\mathbf{f}, \mathbf{v}), \\ (\nabla\cdot\mathbf{u}_h, q_h) &=& 0 \end{array}\right. \tag{5}$$

with $\gamma \geq 0$ is a stabilization parameter and the corresponding term can be viewed as adding a consistent term to the momentum equation, since in most of the finite element $\nabla\cdot\mathbf{u}_h \neq 0$, plays a role to penalize the mass conservation.

Here the bilinear form b_s is defined by

1. $b_s(\mathbf{b}; \mathbf{u}_h, \mathbf{v}_h) = (\mathbf{b}\cdot\nabla\mathbf{u}_h, \mathbf{v}_h)$ with $\nabla\cdot\mathbf{b} = 0$
2. $b_s(\mathbf{b}; \mathbf{u}_h, \mathbf{v}_h) = \frac{1}{2}\big\{(\mathbf{b}\cdot\nabla\mathbf{u}_h, \mathbf{v}_h) - (\mathbf{b}\cdot\nabla\mathbf{v}_h, \mathbf{u}_h)\big\}$.

Grad-div stabilization can be used with any finite element choice and meshes. Our interest lies in the spaces of weakly differentiable pointwise divergence-free functions and discretely divergence-free functions which are defined as follows, respectively

$$\begin{aligned} V_0 &= \big\{\mathbf{v} \in H_0^1(\Omega)^d \ : \ \nabla\cdot\mathbf{v} = 0\big\} \\ V_{0,h} &= \big\{\mathbf{v}_h \in V_h \ : \ (\nabla\cdot\mathbf{v}_h, q_h) = 0, \quad \text{for all } q_h \in Q_h\big\}. \end{aligned}$$

It is to be noted that the discretely divergence-free function does not have to be divergence-free. This means that $V_{0,h} \not\subset V_0$ even if $V_h \subset V$. The reason is that the divergence-free element might

results in violation of the mass conservation. There stability relies on the choice of finite element spaces and special mesh construction. To derive appropriate values of the stabilization parameter γ, the space of divergence-free and discretely divergence-free functions $V_{00,h} \subset V_{0,h} \cap V_0$ will be used with particular emphasis on the conditions whether the space $V_{00,h}$ posses optimal approximation properties or not.

Definition: Consider a sequence of quasi-uniform meshes with characteristic mesh size h and the corresponding spaces $V_{00,h}$. If for all $v \in V_0 \cap H^{k+1}(\Omega)^d$ there exists a sequence of $v_h \in V_{00,h}$ with

$$\|\nabla(\mathbf{v} - \mathbf{v}_h)\|_0 \leq C_{V_{00,h}} h^k |\mathbf{v}|_{k+1} \tag{6}$$

with $C_{V_{00,h}}$ independent of h, then the sequence of spaces $V_{00,h}$ is said to possess optimal approximation properties (w.r.t. the space V_0).

3. Velocity estimates and grad-div parameters

This section details the main results of the paper. In particular, only the minimization of the H^1-norm of velocity is considered to study the optimality of the stabilization parameters. Two different cases on the reaction coefficient σ are taken into account, i.e., $\sigma = 0$ and $\sigma > 0$.

Theorem 3.1. *Let $\mathbf{f} \in H^{-1}(\Omega)$ is given $(\mathbf{u}, p)$ be the solution of the continuous (3) and $(\mathbf{u}_h, p_h)$ be the solution of the discrete problem (5). Then, the following estimates in the $L^2(\Omega)$-norm of the gradient of the velocity holds*

$$\begin{aligned}\|\nabla(\mathbf{u} - \mathbf{u}_h)\|_0^2 \leq \inf_{\mathbf{w}_h \in V_{0,h}} \Big\{ \mathcal{C}_g \|\nabla(\mathbf{u} - \mathbf{w}_h)\|_0^2 + \mathcal{C}_r \|\mathbf{u} - \mathbf{w}_h\|_0^2 + \mathcal{C}_d \|\nabla \cdot \mathbf{w}_h\|_0^2 \Big\} \\ + \mathcal{C}_p \inf_{q_h \in Q_h} \|p - q_h\|_0^2 \end{aligned} \tag{7}$$

where the constants $\mathcal{C}_g$, $\mathcal{C}_r$, $\mathcal{C}_d$, $\mathcal{C}_p$ that depends on the problem data are defined as follows:

***Case I**: Consider $\sigma > 0$. For $b_s(\mathbf{b}; \mathbf{u}_h, \mathbf{v}_h) = (\mathbf{b} \cdot \nabla \mathbf{u}_h, \mathbf{v}_h)$ with $\nabla \cdot \mathbf{b} = 0$, constants on the right hand side of (7) are given by*

$$\mathcal{C}_g = 4 + \frac{2\|\mathbf{b}\|_\infty^2}{\nu\sigma}, \qquad \mathcal{C}_r = \frac{2\sigma}{\nu}, \qquad \mathcal{C}_d = \frac{2\gamma}{\nu}, \qquad \mathcal{C}_p = \frac{2}{\gamma}. \tag{8}$$

Similarly, for $b_s(\mathbf{b}; \mathbf{u}_h, \mathbf{v}_h) = \frac{1}{2}\big\{(\mathbf{b} \cdot \nabla \mathbf{u}_h, \mathbf{v}_h) - (\mathbf{b} \cdot \nabla \mathbf{v}_h, \mathbf{u}_h)\big\}$, one have

$$\mathcal{C}_g = \left(6 + \frac{\|\mathbf{b}\|_\infty^2}{\nu\sigma}\right), \qquad \mathcal{C}_r = \left(\frac{4\sigma}{\nu} + \frac{2\|\mathbf{b}\|_\infty^2}{\nu^2}\right), \qquad \mathcal{C}_d = \frac{4\gamma}{\nu}, \qquad \mathcal{C}_p = \frac{4}{\nu\gamma}. \tag{9}$$

***Case II**: Consider $\sigma = 0$. The constants on the right hand side of (7) are defined by*

$$\mathcal{C}_g = \left(6 + \frac{C\|\mathbf{b}\|_\infty^2}{\nu^2}\right), \qquad \mathcal{C}_r = 0, \qquad \mathcal{C}_d = \frac{4\gamma}{\nu}, \qquad \mathcal{C}_p = \frac{4}{\nu\gamma}. \tag{10}$$

Proof. For arbitrary $\mathbf{w}_h \in V_{0,h}$, consider the error splitting

$$\mathbf{u} - \mathbf{u}_h = (\mathbf{u} - \mathbf{w}_h) + (\mathbf{w}_h - \mathbf{u}_h) := \eta + \boldsymbol{\xi}_h.$$

Then, the triangular inequality and Young's inequality gives

$$\|\nabla \mathbf{u} - \nabla \mathbf{u}_h\|_0^2 \leq 2\|\nabla \eta\|_0^2 + 2\|\nabla \boldsymbol{\xi}_h\|_0^2. \tag{11}$$

Subtracting (5) and (3) yield the following error equation

$$\begin{aligned}&\nu(\nabla \boldsymbol{\xi}_h, \nabla \mathbf{v}_h) + b_s(\mathbf{b}; \boldsymbol{\xi}_h, \mathbf{v}_h) + \sigma(\boldsymbol{\xi}_h, \mathbf{v}_h) + \gamma(\nabla \cdot \boldsymbol{\xi}_h, \nabla \cdot \mathbf{v}_h) \\ &\quad = -\nu(\nabla \eta, \nabla \mathbf{v}_h) - b_s(\mathbf{b}; \eta, \mathbf{v}_h) - \sigma(\eta, \mathbf{v}_h) - \gamma(\nabla \cdot \eta, \nabla \cdot \mathbf{v}_h) + (p, \nabla \cdot \mathbf{v}_h).\end{aligned}$$

Setting $\mathbf{v}_h = \boldsymbol{\xi}_h$ and using $(\nabla \cdot \boldsymbol{\xi}_h, q_h) = 0$ for any $q_h \in Q_h$, the error equation becomes for any $q_h \in Q_h$

$$\begin{aligned}&\nu\|\nabla\boldsymbol{\xi}_h\|_0^2 + \sigma\|\boldsymbol{\xi}_h\|_0^2 + \gamma\|\nabla\cdot\boldsymbol{\xi}_h\|_0^2\\ &\quad = -\nu(\nabla\eta, \nabla\boldsymbol{\xi}_h) - b_s(\mathbf{b};\eta,\boldsymbol{\xi}_h) - \sigma(\eta,\boldsymbol{\xi}_h) - \gamma(\nabla\cdot\eta, \nabla\cdot\boldsymbol{\xi}_h) + (p-q_h, \nabla\cdot\boldsymbol{\xi}_h). \end{aligned} \tag{12}$$

The terms on the right-hand side of (12) will be estimated separately. Applying the Cauchy-Schwarz inequality and Young's inequality, one gets

$$\begin{aligned}\nu\|\nabla\boldsymbol{\xi}_h\|_0^2 + \sigma\|\boldsymbol{\xi}_h\|_0^2 + \gamma\|\nabla\cdot\boldsymbol{\xi}_h\|_0^2 \le \nu\|\nabla\eta\|_0^2 + \sigma\|\eta\|_0^2 + \gamma\|\nabla\cdot\eta\|_0^2 + 2\big|b_s(\mathbf{b};\eta,\boldsymbol{\xi}_h)\big|\\ + 2\big|(p-q_h, \nabla\cdot\boldsymbol{\xi}_h)\big|. \end{aligned} \tag{13}$$

The estimate of the last term on the right-hand side of (12) uses again the Cauchy-Schwarz and Young's inequality

$$2\big|(p-q_h, \nabla\cdot\boldsymbol{\xi}_h)\big| \le 2\gamma^{-1/2}\,\|p-q_h\|_0\,\gamma^{1/2}\,\|\nabla\cdot\boldsymbol{\xi}_h\|_0 \le \gamma^{-1}\|p-q_h\|_0^2 + \gamma\|\nabla\cdot\boldsymbol{\xi}_h\|_0^2. \tag{14}$$

for all $q_h \in Q_h$. For the estimates of the convective term, two different cases of σ are taken into account with the different representations of the bilinear form b_s. First consider the case $\sigma \neq 0$, then using the definitions of b_s gives, respectively

$$2\big|b_s(\mathbf{b};\eta,\boldsymbol{\xi}_h)\big| = 2(\mathbf{b}\cdot\nabla\eta, \boldsymbol{\xi}_h) \le 2\|\mathbf{b}\|_\infty\|\nabla\eta\|_0\|\boldsymbol{\xi}_h\|_0 \le \frac{\|\mathbf{b}\|_\infty^2}{\sigma}\|\nabla\eta\|_0^2 + \sigma\|\boldsymbol{\xi}_h\|_0^2 \tag{15}$$

and

$$\begin{aligned}2\big|b_s(\mathbf{b};\eta,\boldsymbol{\xi}_h)\big| &= \big|(\mathbf{b}\cdot\nabla\eta, \boldsymbol{\xi}_h) - (\mathbf{b}\cdot\nabla\boldsymbol{\xi}_h, \eta)\big| \le \|\mathbf{b}\|_\infty\,\|\nabla\eta\|_0\,\|\boldsymbol{\xi}_h\|_0 + \|\mathbf{b}\|_\infty\,\|\nabla\boldsymbol{\xi}_h\|_0\|\boldsymbol{\xi}_h\|_0\\ &\le \frac{\|\mathbf{b}\|_\infty^2}{4\sigma}\|\nabla\eta\|_0^2 + \sigma\|\boldsymbol{\xi}_h\|_0^2 + \frac{\|\mathbf{b}\|_\infty^2}{2\nu}\|\eta\|_0^2 + \frac{\nu}{2}\|\nabla\boldsymbol{\xi}_h\|_0^2. \end{aligned} \tag{16}$$

Inserting (14) and (15) into (13) gives

$$\|\nabla\boldsymbol{\xi}_h\|_0^2 \le \left(1 + \frac{\|\mathbf{b}\|_\infty^2}{\nu\sigma}\right)\|\nabla\eta\|_0^2 + \frac{\sigma}{\nu}\|\eta\|_0^2 + \frac{\gamma}{\nu}\|\nabla\cdot\eta\|_0^2 + \frac{1}{\nu\gamma}\inf_{q_h\in Q_h}\|p-q_h\|_0^2.$$

Hence, (11) implies

$$\|\nabla(\mathbf{u}-\mathbf{u}_h)\|_0^2 \le 4\left(1 + \frac{\|\mathbf{b}\|_\infty^2}{2\nu\sigma}\right)\|\nabla\eta\|_0^2 + \frac{2\sigma}{\nu}\|\eta\|_0^2 + \frac{2\gamma}{\nu}\|\nabla\cdot\eta\|_0^2 + \frac{2}{\nu\gamma}\inf_{q_h\in Q_h}\|p-q_h\|_0^2$$

which gives (7) together with the constants (8).

Collecting the estimates from (14) and (16) into (13)

$$\begin{aligned}\|\nabla\boldsymbol{\xi}_h\|_0^2 \le 2\|\nabla\eta\|_0^2 + \frac{2\sigma}{\nu}\|\eta\|_0^2 + \frac{2\gamma}{\nu}\|\nabla\cdot\eta\|_0^2 + \frac{\|\mathbf{b}\|_\infty^2}{2\nu\sigma}\|\nabla\eta\|_0^2 + \frac{\|\mathbf{b}\|_\infty^2}{\nu^2}\|\eta\|_0^2\\ + \frac{2}{\nu\gamma}\inf_{q_h\in Q_h}\|p-q_h\|_0^2. \end{aligned}$$

Eq.(11) implies

$$\begin{aligned}\|\nabla(\mathbf{u}-\mathbf{u}_h)\|_0^2 \le \left(6 + \frac{\|\mathbf{b}\|_\infty^2}{\nu\sigma}\right)\|\nabla\eta\|_0^2 + \left(\frac{4\sigma}{\nu} + \frac{2\|\mathbf{b}\|_\infty^2}{\nu^2}\right)\|\eta\|_0^2 + \frac{4\gamma}{\nu}\|\nabla\cdot\eta\|_0^2\\ + \frac{4}{\nu\gamma}\inf_{q_h\in Q_h}\|p-q_h\|_0^2, \qquad \forall\mathbf{w}_h \in V_{0,h} \end{aligned}$$

Hence, one can obtain the required estimates (7) with the constants from (9).

Consider now the second case where $\sigma = 0$. Applying Hölder's inequality followed by the Poincaré and Young's inequality, one get the estimates of the convective term

$$b_s(\mathbf{b};\eta,\boldsymbol{\xi}_h) \le C\|\mathbf{b}\|_\infty\|\nabla\eta\|_0\|\nabla\boldsymbol{\xi}_h\|_0 \le \frac{C\|\mathbf{b}\|_\infty^2}{\nu}\|\nabla\eta\|_0^2 + \frac{\nu}{4}\|\nabla\boldsymbol{\xi}_h\|_0^2.$$

Using this estimate, $\sigma = 0$, (14) into (13) to get

$$\|\nabla \boldsymbol{\xi}_h\|_0^2 \leq \left(2 + \frac{C\|\mathbf{b}\|_\infty^2}{\nu^2}\right) \|\nabla \eta\|_0^2 + \frac{2\gamma}{\nu}\|\nabla \cdot \eta\|_0^2 + \frac{2}{\gamma\nu} \inf_{q_h \in Q_h} \|p - q_h\|_0^2.$$

Hence, using this estimate in (11) yields the statement of theorem with the constants defined in (10). □

As pointed out in the grad-div stabilization applied to the Stokes problem [13], the key point of the analysis consists in tracking the divergence error to the final estimates of Theorem 3.1, which allows to study the consequences of the error bounds (7) on the choice of the parameters γ for the cases of pointwise divergence-free subspace of velocity space have or does not have optimal approximation properties.

3.1. Taylor-Hood elements

Corollary 3.2. *Consider* $(V_h, Q_h) = \left((P_k)^d, P_{k-1}\right)$ *on quasi-uniform meshes and* $(\mathbf{u}, p) \in H^{k+1}(\Omega)^d \times H^k(\Omega)$.

The estimates are distinguished into different categories depends on the existence of the optimal approximation properties, the reaction coefficient σ *and bilinear form* b_s.

Case 1: *First consider the general case where the space* $V_{00,h}$ *does not posses the optimal approximation properties. In this case the estimates of Theorem 3.1 takes the form*

$$\|\nabla \mathbf{u} - \nabla \mathbf{u}_h\|_0^2 \leq \left[\mathcal{C}_g + \mathcal{C}_r h^2 + \mathcal{C}_d\right] C_{V_{0,h}}^2 h^{2k} |\mathbf{u}|_{k+1}^2 + \mathcal{C}_p C_{Q_h}^2 h^{2k} |p|_k^2. \tag{17}$$

Case 2: *If the space* $V_{00,h}$ *posses the optimal approximation properties, the estimates* (7) *gives*

$$\begin{aligned}\|\nabla \mathbf{u} - \nabla \mathbf{u}_h\|_0^2 \leq \min\left\{\left[\left[\mathcal{C}_g + \mathcal{C}_r h^2 + \mathcal{C}_d\right] C_{V_{0,h}}^2, \mathcal{C}_g + \mathcal{C}_r h^2\right] C_{V_{00,h}}^2\right\} h^{2k} |\mathbf{u}|_{k+1}^2 \\ + \mathcal{C}_p C_{Q_h}^2 h^{2k} |p|_k^2.\end{aligned} \tag{18}$$

Note that, the constants $\mathcal{C}_g$, $\mathcal{C}_r$, $\mathcal{C}_d$, *and* $\mathcal{C}_p$ *that appears on the right-hand side of both estimates are defined in* (8)–(10) *for different cases. Furthermore, the constants* $C_{Q_h}, C_{V_0,h}$ *and* $C_{V_{00,h}}$ *appears in all the estimates are the interpolation estimates constants.*

Proof. The proof follows the same steps as that of [13, Corollary 1]. □

In the remainder of this section, the two cases will be discussed in more details. Firstly the case that the space $V_{00,h}$ doesn't have optimal approximation properties. Following the elementary calculus to compute the minimum by considering the right-hand side of the estimates (17) as a function depending on γ, one gets the optimal value

$$\gamma_{\text{opt}} \approx \frac{C_{Q_h}|p|_k}{C_{V_{0,h}}|\mathbf{u}|_{k+1}}. \tag{19}$$

It is to be noted that the parameter γ_{opt} is similar to the one that is obtained for the Stokes problem [13], and, with respect to ν and h, the standard parameter choice $\gamma = \mathcal{O}(1)$ is recovered. Inserting γ_{opt} into (17), leads to the error estimates of the form

$$\|\nabla(\mathbf{u} - \mathbf{u}_h)\|_0 \leq h^k \left(\left(\mathcal{C}_g + \mathcal{C}_r h^2\right) C_{V_{0,h}}^2 |\mathbf{u}|_{k+1}^2 + \frac{2\varepsilon}{\nu} C_{V_{0,h}} C_{Q_h} |\mathbf{u}|_{k+1} |p|_k\right)^{1/2} \tag{20}$$

with $\varepsilon = 2$ or 4 depending on cases of Theorem 3.1.

Consider now the case where the space $V_{00,h}$ has optimal approximation properties. In order to obtain good value of parameter γ, follow the criteria of Stokes problem by considering the contribution of the pressure error equals to the maximum possible contribution of the velocity error. This criterion for the estimates (18) leads to the estimates

$$\gamma_{\text{good}} \approx \frac{\varepsilon C_{Q_h}^2 |p|_k^2}{\nu\left(\mathcal{C}_g + \mathcal{C}_r h^2\right) C_{V_{00,h}}^2 |\mathbf{u}|_{k+1}^2}. \tag{21}$$

From the definitions of the constants (8), (9) and (9), it can be observed that the contribution of the term $\nu(\mathcal{C}_g + \mathcal{C}_r)$ is large. Hence, if $|p|_k^2/|\mathbf{u}|_{k+1}^2$ is small, then one can conclude that the decrease in viscosity does not influence the value of optimal parameter γ. In contrast, the value of the optimal γ increases by decreasing the parameter ν for the Stokes problem. This observation is also verified in the numerical studies presented in Section 4. Inserting (21) into (18) gives

$$\|\nabla(\mathbf{u} - \mathbf{u}_h)\|_0 \leq \varepsilon \left(\mathcal{C}_g + \mathcal{C}_r h^2\right)^{1/2} C_{V_{00,h}} h^k |\mathbf{u}|_{k+1} \tag{22}$$

with $\varepsilon = \sqrt{8}$ or $\sqrt{2}$ depending on $\sigma = 0$ or $\sigma = 1$, respectively.

For estimates (20) and (22), since $\mathcal{C}_g$ and $\mathcal{C}_r$ depends on ν^{-1} (even ν^{-2} when $\sigma = 0$), it is predicted that a decrease in the viscosity would results in the large velocity errors.

3.2. Mini elements

It is well known that the use of equal-order finite element pair $((P_k)^d, P_k)$ does not satisfy the inf-sup condition (4). In order to overcome the difficulty, a PSPG term have to be added to the discrete formulation (5), see e.g., [15, 16]. The use of MINI element (P_k^{bub}, P_k) is equivalent to apply the PSPG stabilization, with a special choice of the PSPG parameter [17].

Corollary 3.3. *Consider* $(V_h, Q_h) = \left((P_k^{\text{bub}})^d, P_k\right)$ *on quasi-uniform meshes and* $(\mathbf{u}, p) \in H^{k+1}(\Omega)^d \times H^{k+1}(\Omega)$.

Similarly as for the Taylor-Hood element, two cases depending on the the approximation properties of the space $V_{00,h}$ are detailed in the following.

Case 1: A-priori estimates (7), for the general case where the space $V_{00,h}$ does not have optimal approximation properties, has the form

$$\|\nabla(\mathbf{u} - \mathbf{u}_h)\|_0^2 \leq \left[\mathcal{C}_g + h^2\mathcal{C}_r + \mathcal{C}_d\right] C_{V_{0,h}}^2 h^{2k} |\mathbf{u}|_{k+1}^2 + \mathcal{C}_p C_{Q_h}^2 h^{2k+2} |p|_{k+1}^2. \tag{23}$$

Case 2: In the case that the space $V_{00,h}$ has optimal approximation properties, the a-priori estimates (7) becomes

$$\begin{aligned}\|\nabla(\mathbf{u} - \mathbf{u}_h)\|_0^2 \leq \min\left\{\left[\left(\mathcal{C}_g + \mathcal{C}_r h^2 + \mathcal{C}_d\right) C_{V_{0,h}}^2, \mathcal{C}_g + \mathcal{C}_r h^2\right] C_{V_{00,h}}^2\right\} h^{2k} |\mathbf{u}|_{k+1}^2 \\ + \mathcal{C}_p C_{Q_h}^2 h^{2k+2} |p|_{k+1}^2\end{aligned} \tag{24}$$

with $\mathcal{C}_g$, $\mathcal{C}_r$, $\mathcal{C}_d$ and $\mathcal{C}_p$ from Theorem 3.1. One can note here that in both estimates there is a dependence of the parameters on the mesh width h which comes from the equal-order finite element pairs of velocity and pressure.

Using the same idea as in the Taylor-Hood element for finding the parameters γ_{opt} and γ_{good}, depending on the approximation properties of the space $V_{00,h}$, one arrives at

$$\gamma_{\text{opt}} = \frac{h C_{Q_h} |p|_{k+1}}{C_{V_{0,h}} |\mathbf{u}|_{k+1}}, \qquad \gamma_{\text{good}} = \frac{\varepsilon h^2 C_{Q_h}^2 |p|_{k+1}^2}{\nu \left(\mathcal{C}_g + \mathcal{C}_r h^2\right) C_{V_{00,h}}^2 |\mathbf{u}|_{k+1}^2}. \tag{25}$$

In these cases, one expects a dependence of the optimal γ on the mesh width h, but is independent of the parameter ν due to the definitions of $\mathcal{C}_g$ and $\mathcal{C}_r$. Inserting γ_{opt} and γ_{good} into (23) and (24), respectively, gives the following estimates

$$\|\nabla(\mathbf{u} - \mathbf{u}_h)\|_0 \leq h^k \left(\left(\mathcal{C}_g + h^2\mathcal{C}_r\right) C_{V_{0,h}}^2 |\mathbf{u}|_{k+1}^2 + \frac{2h\varepsilon}{\nu} C_{V_{0,h}} C_{Q_h} |p|_{k+1} |\mathbf{u}|_{k+1}\right)^{1/2} \tag{26}$$

and

$$\|\nabla(\mathbf{u} - \mathbf{u}_h)\|_0 \leq \varepsilon h^k \left(\mathcal{C}_g + h^2\mathcal{C}_r\right)^{1/2} C_{V_{0,h}} |\mathbf{u}|_{k+1}. \tag{27}$$

A similar observation as for the Taylor-Hood element can be made for the MINI element that a decrease in the viscosity would results in the large velocity errors, since the constant $\mathcal{C}_g$ and $\mathcal{C}_r$ depends on ν^{-1}.

4. Numerical studies

This section presents the numerical results consisting of two examples. The first considered in a unit square $(0,1)^2$ for which the analytic solution is known. In this example, our interest lies to compute and compare the influence of the optimal γ with the theoretical results presented in previous section. The second example is the well known steady-state flow past a circular cylinder. The goal of this example is to numerically investigate the effect of the parameter γ in grad-div stabilization applied to Navier-Stokes equation. All numerical simulations were performed with the finite element code MooNMD [18].

4.1. Example with known analytic solution

Consider the problem (2) on $\Omega = (0,1)^2$, $\mathbf{b} = \mathbf{u}$ and $\sigma = 1$ or $\sigma = 0$. Choose $\mathbf{f}$ and the boundary conditions such that

$$\mathbf{u}(\mathbf{x},\mathbf{y}) = \begin{pmatrix} \cos(2\pi\mathbf{y}) \\ \sin(2\pi\mathbf{x}) \end{pmatrix}$$

and three different pressure solutions which serves as pressure field

$$p_1 = \sin(2\pi\mathbf{y}), \quad p_2 = \sin(8\pi\mathbf{y}), \quad p_3 = 10^4 \sin(2\pi\mathbf{y}).$$

Note that, for each pressure function, the source term is different. In the numerical studies, the viscosity $\nu \in \{1, 10^{-1}, 10^{-3}, 10^{-6}\}$ were used and the stabilization parameter γ varies in a wide range from 10^{-3} to 10^4.

For the case where the pointwise divergence-free subspace of the velocity space has optimal approximation properties, we will use the scaling factor $\theta_{\nu,h}$ which is defined for $\sigma = 1$ and $\sigma = 0$, respectively,

$$\theta_{\nu,h} = \begin{cases} \frac{4}{6\nu+1+2h^2\left(2+\frac{1}{\nu}\right)} & \text{if } \sigma = 1 \\ \frac{4}{6\nu+\frac{Ch^2}{\nu}} & \text{if } \sigma = 0. \end{cases} \tag{28}$$

Note that the scaling parameter $\theta_{\nu,h}$ decreases by decreasing the viscosity or the mesh width. This fact will also be taken into account in numerical simulations to argue the behavior of the stabilization parameter γ.

In order to compare the results with the Stokes problem from [13], numerical studies for this example were performed on uniformly refined grids using the Taylor-Hood element the MINI element [19]. It is known from [20] that, the pointwise divergence-free subspace $(P_2)^2$ of the velocity space has optimal approximation properties on the barycenter-refined mesh. Also, the pointwise divergence-free subspace of $\left(P_1^{\text{bub}}\right)^2$ on union jack type meshes has optimal approximation properties.

For simplicity of presentation, the parameters proposed by the theoretical results in previous section will be denoted by γ_{good} and by optimal γ that corresponds to the best results obtained in the numerical simulations.

4.1.1. $((P_2)^2, P_1)$ Taylor-Hood element on barycenter-refined grids

First consider the Taylor-Hood element on the barycentric refined uniform mesh, where the divergence-free subspace of the velocity space posses optimal approximation properties. In this case, (19) will be taken into account and the good choice of γ satisfies

$$\gamma_{\text{good}} \approx \theta_{\nu,h} C_0 \frac{|p|_2^2}{|\mathbf{u}|_3^2} = \theta_{\nu,h} C_0 \begin{cases} \frac{1}{2\pi^2} & \text{for } p = p_1 \\ \frac{128}{\pi^2} & \text{for } p = p_2 \\ \frac{10^8}{2\pi^2} & \text{for } p = p_3 \end{cases} \tag{29}$$

where C_0 is a constant which has to be specified.

In Fig. 1 and 2, the $H^1(\Omega)$ errors of the velocity are plotted against the grad-div stabilization parameters γ for $\sigma = 1$ and $\sigma = 0$, respectively. From the choice (29), one expect small values of the optimal parameters by decreasing the viscosity parameter ν. This effect can be seen also in the

numerical simulations. Equation (29) also suggests an increase in the optimal γ if $|p|_2$ is increases. This behavior can be well observed in the numerical simulations by comparing the optimal γ for p_1 and p_2 (similarly p_2 and p_3). Furthermore, large values of the optimal γ for larger $|p|_2^2$ and h independence are predicted from (29). Both observations are confirmed numerically.

Since the error estimates (22) shows a dependence on ν^{-1} (or ν^{-2}, one expect to see an increase of the error for optimal γ if ν decreases. This increase can be observed in all simulations.

The same prediction concerning the accuracy of the computed solution for the Stokes problem [13] comparing the errors of optimal γ and the standard choice $\gamma = 1$ can be observed here. That is, errors computed with optimal γ are smaller by several orders of magnitude than the errors obtained by standard parameter $\gamma = 1$. One can see this observation in the case where $|p|_2^2$ is large, i.e., for p_3. Finally, there is almost no difference between the computed solution with $\sigma = 1$ and $\sigma = 0$.

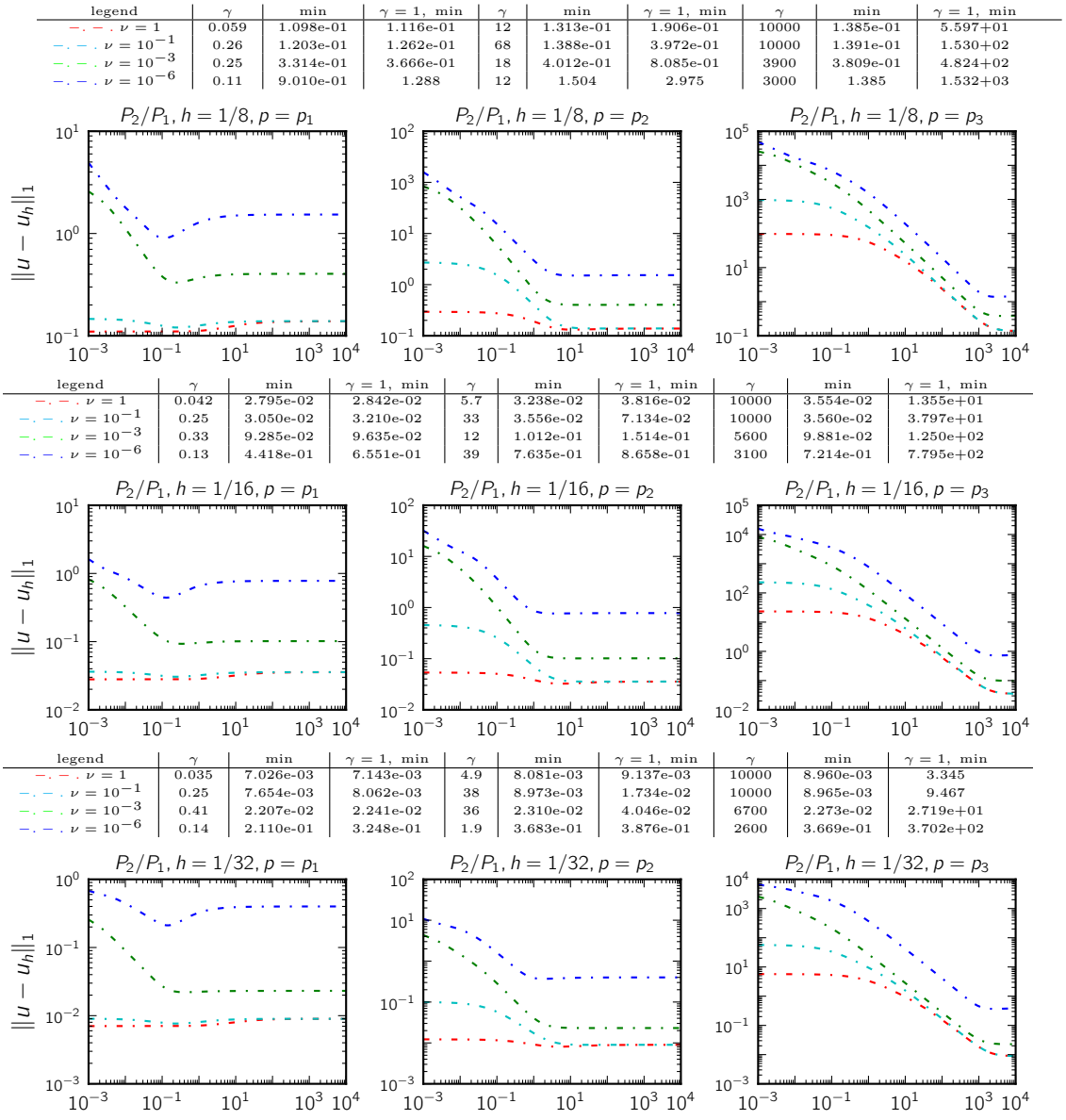

Figure 1: Errors in the H^1-norm of velocity vs. grad-div stabilization parameter γ with $\sigma = 1$ on successive refinements of barycenter–refined uniform meshes.

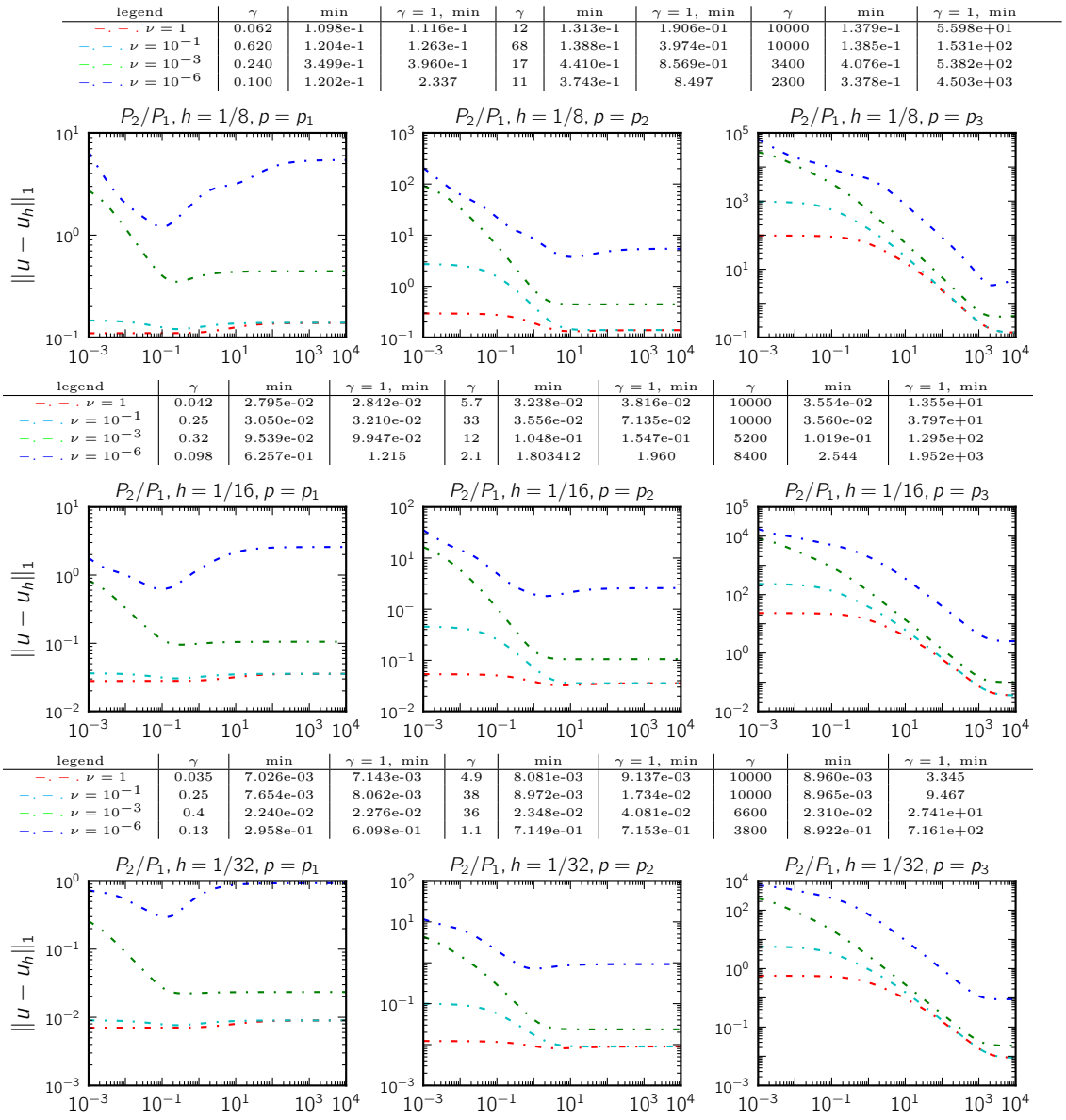

Figure 2: Errors in the H^1-norm of velocity vs. grad-div stabilization parameter γ with $\sigma = 0$ on successive refinements of barycenter–refined uniform meshes.

4.1.2. $((P_2)^2, P_1)$ *Taylor-Hood element on Delauney-generated triangulations*

In this case, the pointwise divergence-free subspace of velocity does not have the optimal approximation properties. Hence, the parameter choice (19) is applied which is similar to the γ_{good} for the Stokes problem, one can obtains

$$\gamma_{\text{good}} \approx \begin{cases} \frac{C_0}{\sqrt{8}\pi} & \text{for } p = p_1 \\ \frac{C_0\sqrt{32}}{\pi} & \text{for } p = p_2 \\ \frac{C_0 10^4}{\sqrt{8}\pi} & \text{for } p = p_3. \end{cases} \tag{30}$$

Figures 3 and 4 plots the $H^1(\Omega)$ errors for the velocity against the stabilization parameters γ for successively refined Delauney-generated triangulations with $h \in \{1/8,\ 1/16,\ 1/32\}$. Again from (30), one does not expect a dependence of optimal parameter γ on the viscosity ν which can also be observed in the numerical simulations for p_1 and p_2. Similar to the case where the subspace has

optimal approximation properties (Eq. (29), and figures 1 and 2) one can observe a small increase in the optimal values of γ between p_1 and p_2 which are confirmed by comparing the values of γ in the first and second column. Moreover, much higher values of optimal parameter for the large $|p|_2$ (for p_3) and h-independence of the optimal stabilization parameter are observed from (30). Both prediction can be confirmed from the numerical simulations.

Comparing the results for $\sigma = 1$ and $\sigma = 0$ in figures 3 and 4, one can see for $\nu = 0.1$ the influence of large value of stabilization parameter results in the numerical instabilities.

Finally, also an increase in the error estimates (20) can be seen by decreasing ν. This increase can be confirmed from the numerical simulations as well.

legend	γ	min	$\gamma = 1$, min	γ	min	$\gamma = 1$, min	γ	min	$\gamma = 1$, min
$\nu = 1$	0.096	1.341e-01	1.353e-01	6.7	1.572e-01	2.217e-01	10000	3.597e-01	5.395e+01
$\nu = 10^{-1}$	0.21	1.435e-01	1.565e-01	5.0	2.202e-01	4.007e-01	10000	3.654e-01	1.389e+02
$\nu = 10^{-3}$	0.31	3.755e-01	4.205e-01	4.7	5.597e-01	8.534e-01	10000	6.630e-01	6.249e+02
$\nu = 10^{-6}$	0.33	4.577e-01	5.238e-01	3.8	7.090e-01	9.938e-01	10000	9.391e-01	8.207e+02

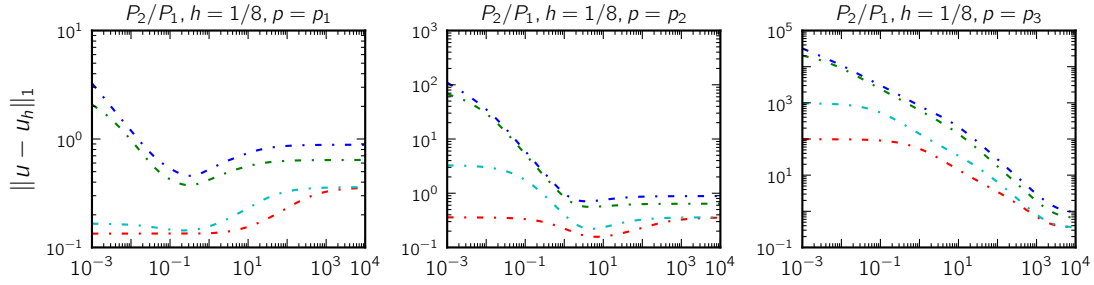

legend	γ	min	$\gamma = 1$, min	γ	min	$\gamma = 1$, min	γ	min	$\gamma = 1$, min
$\nu = 1$	0.12	3.315e-02	1.353e-01	4.6	3.671e-02	2.217e-01	10000	1.326e-01	5.395e+01
$\nu = 10^{-1}$	0.2	3.459e-02	1.565e-01	3.4	5.595e-02	4.007e-01	10000	1.352e-01	1.389e+02
$\nu = 10^{-3}$	0.17	1.206e-01	4.205e-01	3.5	2.025e-01	8.534e-01	10000	2.359e-01	6.248e+02
$\nu = 10^{-6}$	0.17	2.117e-01	5.238e-01	2.3	3.851e-01	9.938e-01	10000	5.195e-01	8.207e+02

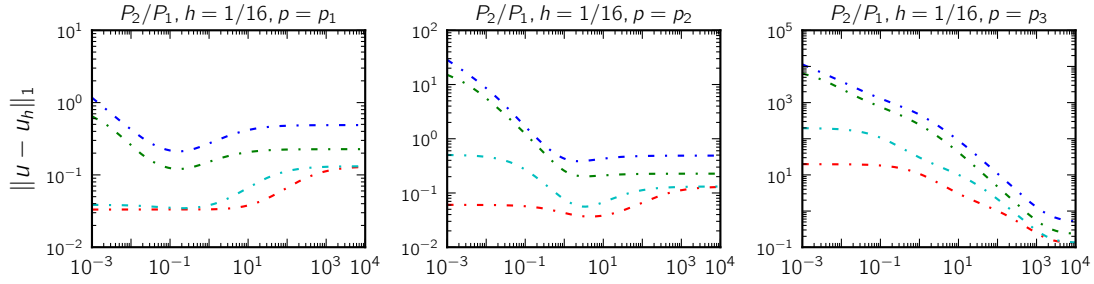

legend	γ	min	$\gamma = 1$, min	γ	min	$\gamma = 1$, min	γ	min	$\gamma = 1$, min
$\nu = 1$	0.092	7.768e-03	7.809e-03	3.5	8.328e-03	8.904e-03	10000	3.903e-02	2.190
$\nu = 10^{-1}$	0.19	8.048e-03	8.7596e-03	2.8	1.242e-02	1.460e-02	10000	4.016e-02	6.017
$\nu = 10^{-3}$	0.13	2.607e-02	3.817e-02	5.2	5.560e-02	8.332e-02	10000	6.080e-02	6.429e+01
$\nu = 10^{-6}$	0.13	8.495e-02	1.2741e-01	3.3	1.832e-01	2.196e-01	10000	2.304e-01	2.281e+02

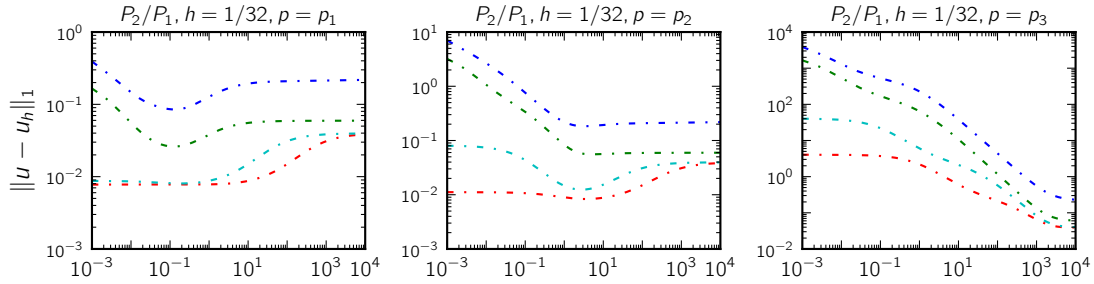

Figure 3: Errors in the H^1-norm of velocity vs. grad-div stabilization parameter γ with $\sigma = 1$ on successive refinements of Delauney–refined uniform meshes.

4.1.3. The MINI element on union jack triangulations

Consider the MINI element $\left((P_1^{\text{bub}})^2, P_1\right)$ on union jack type refined meshes with $h \in \{1/16,\ 1/32,\ 1/64\}$. It is known from [21] that the pointwise divergence-free subspace of the $\left(P_1^{\text{bub}}\right)^2$ velocity on Union jack meshes has optimal approximation properties. In this case, the

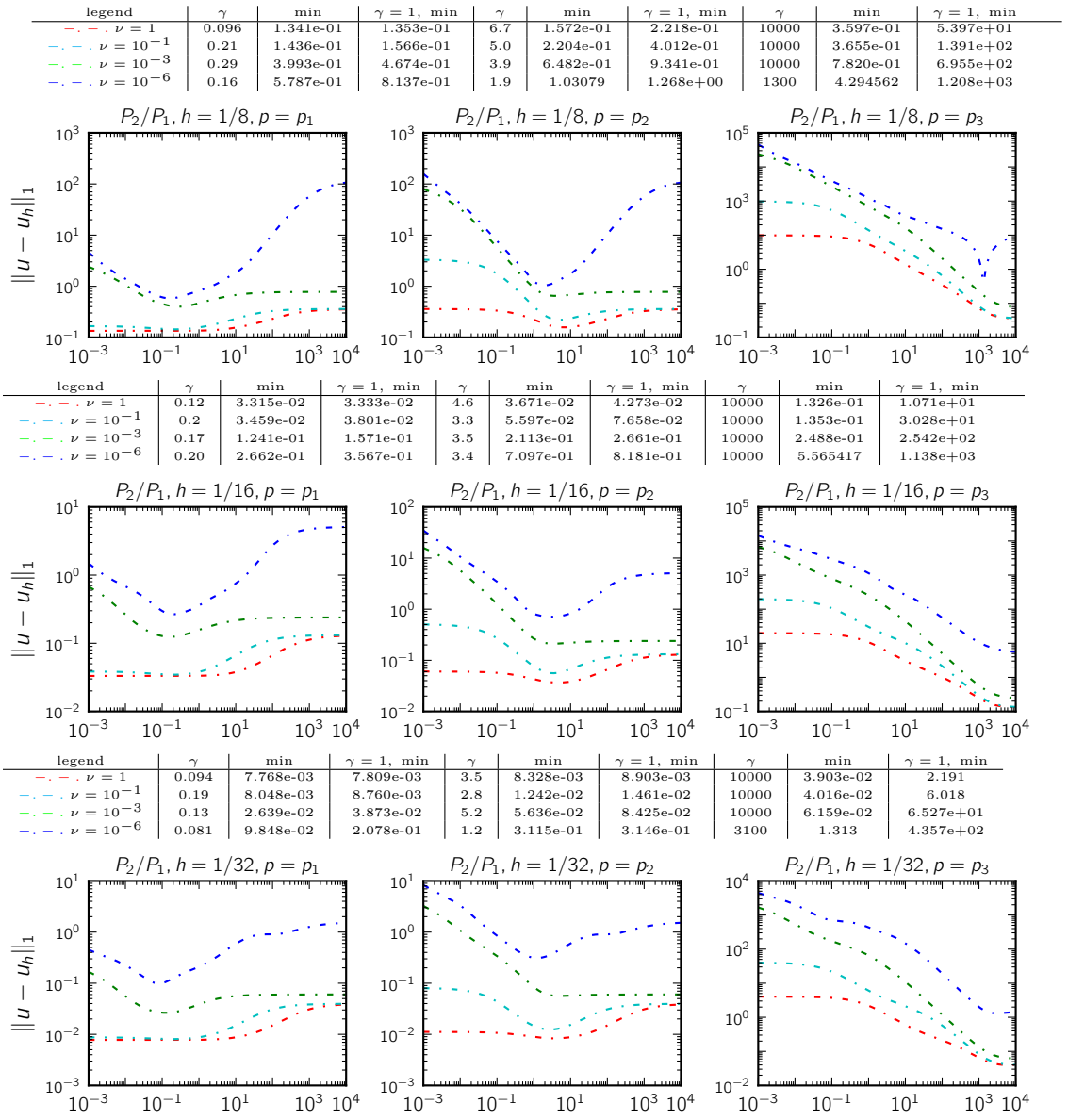

legend	γ	min	$\gamma = 1$, min	γ	min	$\gamma = 1$, min	γ	min	$\gamma = 1$, min
$\nu = 1$	0.096	1.341e-01	1.353e-01	6.7	1.572e-01	2.218e-01	10000	3.597e-01	5.397e+01
$\nu = 10^{-1}$	0.21	1.436e-01	1.566e-01	5.0	2.204e-01	4.012e-01	10000	3.655e-01	1.391e+02
$\nu = 10^{-3}$	0.29	3.993e-01	4.674e-01	3.9	6.482e-01	9.341e-01	10000	7.820e-01	6.955e+02
$\nu = 10^{-6}$	0.16	5.787e-01	8.137e-01	1.9	1.03079	1.268e+00	1300	4.294562	1.208e+03

legend	γ	min	$\gamma = 1$, min	γ	min	$\gamma = 1$, min	γ	min	$\gamma = 1$, min
$\nu = 1$	0.12	3.315e-02	3.333e-02	4.6	3.671e-02	4.273e-02	10000	1.326e-01	1.071e+01
$\nu = 10^{-1}$	0.2	3.459e-02	3.801e-02	3.3	5.597e-02	7.658e-02	10000	1.353e-01	3.028e+01
$\nu = 10^{-3}$	0.17	1.241e-01	1.571e-01	3.5	2.113e-01	2.661e-01	10000	2.488e-01	2.542e+02
$\nu = 10^{-6}$	0.20	2.662e-01	3.567e-01	3.4	7.097e-01	8.181e-01	10000	5.565417	1.138e+03

legend	γ	min	$\gamma = 1$, min	γ	min	$\gamma = 1$, min	γ	min	$\gamma = 1$, min
$\nu = 1$	0.094	7.768e-03	7.809e-03	3.5	8.328e-03	8.903e-03	10000	3.903e-02	2.191
$\nu = 10^{-1}$	0.19	8.048e-03	8.760e-03	2.8	1.242e-02	1.461e-02	10000	4.016e-02	6.018
$\nu = 10^{-3}$	0.13	2.639e-02	3.873e-02	5.2	5.636e-02	8.425e-02	10000	6.159e-02	6.527e+01
$\nu = 10^{-6}$	0.081	9.848e-02	2.078e-01	1.2	3.115e-01	3.146e-01	3100	1.313	4.357e+02

Figure 4: Errors in the H^1-norm of velocity vs. grad-div stabilization parameter γ with $\sigma = 0$ on successive refinements of Delauney–refined uniform meshes.

parameter choice (25) should be used to obtain a good choice for γ, one gets

$$\gamma_{\text{good}} \approx \theta_{\nu,h} h^2 C_0 = \theta_{\nu,h} h^2 C_0 \begin{cases} 1/2 & \text{for } p = p_1 \\ 128 & \text{for } p = p_2 \\ 5 \cdot 10^7 & \text{for } p = p_3. \end{cases} \tag{31}$$

For the sake of brevity, only results with $\sigma = 1$ will be presented. With $\sigma = 0$, almost similar results were obtained.

The results for the numerical simulations are plotted in Fig. 5. From (31), one can see a dependence of the optimal γ on the mesh width h. Hence, the expected decrease in the optimal γ with respect the mesh width h can be confirmed in the numerical simulations. Similarly as for the Taylor-Hood element, a weak or almost no dependence of optimal γ over ν can be seen in the numerical computations which was predicted from (31)

From the estimates (27), it is also expected that the error increases due to the dependence of

ν^{-1}. This effect can be generally observed by comparing the errors for $\nu = 1$, $\nu = 10^{-1}$ and 10^{-3} but not for 10^{-6}. A reason can be that the error stays constant in a wide range of stabilization parameters which also includes the optimal γ.

legend	γ	min	$\gamma = 1$, min	γ	min	$\gamma = 1$, min	γ	min	$\gamma = 1$, min
$\nu = 10^{0}$	1e-03	5.994e-01	6.129e-01	14	3.558e-02	4.504e-02	9700	7.104e-01	1.179e+01
$\nu = 10^{-1}$	1e-03	5.998e-01	6.758e-01	130	3.606e-02	7.338e-02	10000	7.105e-01	4.198e+01
$\nu = 10^{-3}$	0.067	7.128e-01	7.190e-01	51	1.031e-01	1.390e-01	10000	7.203e-01	5.859e+01
$\nu = 10^{-6}$	0.091	7.222e-01	7.318e-01	3.4	2.369e-01	2.543e-01	10000	7.358e-01	5.897e+01

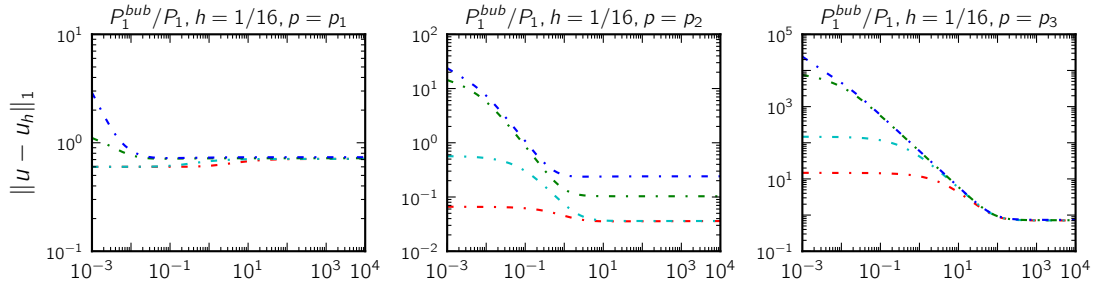

legend	γ	min	$\gamma = 1$, min	γ	min	$\gamma = 1$, min	γ	min	$\gamma = 1$, min
$\nu = 1$	1e-03	3.300-01	3.330e-01	1e-03	2.972e-01	3.042e-01	2300	3.559e-01	2.9073+00
$\nu = 10^{-1}$	1e-03	3.301-01	3.463e-01	0.011	3.036e-01	3.381e-01	9800	3.559e-01	1.0329+01
$\nu = 10^{-3}$	0.21	3.558-01	3.558e-01	5.3	3.574e-01	3.579e-01	9900	3.574e-01	1.4399+01
$\nu = 10^{-6}$	840	3.559-01	3.561e-01	1.1	3.663e-01	3.663e-01	10000	3.672e-01	1.4472+01

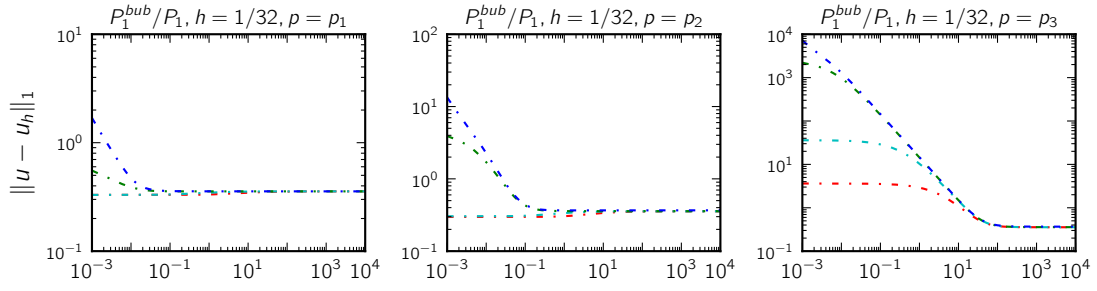

legend	γ	min	$\gamma = 1$, min	γ	min	$\gamma = 1$, min	γ	min	$\gamma = 1$, min
$\nu = 1$	1e-03	1.479e-01	1.515e-01	1e-03	1.479e-01	1.516e-01	560	1.779e-01	7.353e-01
$\nu = 10^{-1}$	1e-03	1.479e-01	1.687e-01	2e-03	1.486e-01	1.688e-01	5100	1.780e-01	2.575e+00
$\nu = 10^{-3}$	3e-03	1.669e-01	1.781e-01	1.5	1.782e-01	1.782e-01	9600	1.782e-01	3.587e+00
$\nu = 10^{-6}$	0.033	1.794e-01	1.825e-01	0.43	1.823e-01	1.826e-01	10000	1.828e-01	3.603e+00

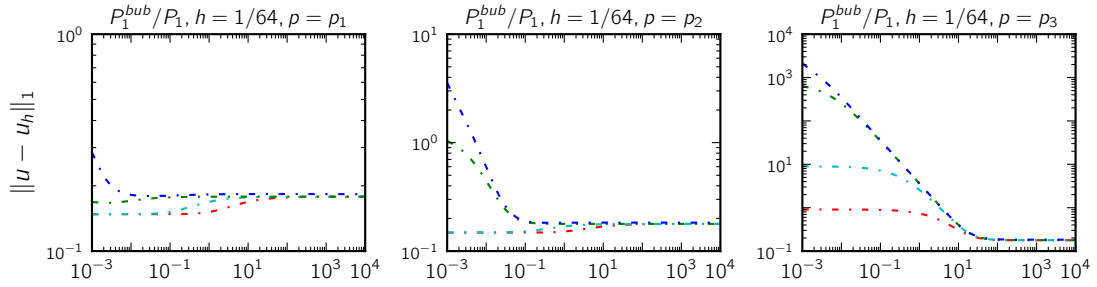

Figure 5: Errors in the H^1-norm of velocity vs. grad-div stabilization parameter γ with $\sigma = 1$ using the MINI element on union jack triangulations with $h \in \{1/16,\ 1/32,\ 1/64\}$.

4.1.4. The MINI on Delauney-generated triangulations

Finally, consider the MINI element on Delauney-generated triangulation where one does not expect the pointwise divergence-free subspace of velocity have the optimal approximation properties. Hence, the stabilization parameter γ_{good} (25) will be taken into account such that

$$\gamma_{\text{good}} \approx hC_0 = \begin{cases} \frac{C_0}{\sqrt{4}}h & \text{for } p = p_1 \\ 8\sqrt{2}C_0 h & \text{for } p = p_2 \\ 5000\sqrt{2}C_0 h & \text{for } p = p_3. \end{cases} \tag{32}$$

Again, one observes a decrease in the optimal γ with respect to the mesh h and no dependence on ν. Both observation are met with the numerical simulation presented in Fig. 6.

A dependence of the error for the optimal γ on ν^{-1} is predicted from the estimates(26) which results in the increase of the velocity error. An increase of the errors for small ν can be observed in Fig. 6.

legend	γ	min	$\gamma = 1$, min	γ	min	$\gamma = 1$, min	γ	min	$\gamma = 1$, min
$\nu = 1$	1e-03	6.248e-01	6.351e-01	0.041	6.263e-01	6.358e-01	860	1.29	1.611e+01
$\nu = 10^{-1}$	3e-03	6.260e-01	7.353e-01	0.24	6.850e-01	7.395e-01	65	2.27	4.160e+01
$\nu = 10^{-3}$	0.033	7.801e-01	1.316133	0.24	1.04010	1.315958	10000	2.89	5.986e+01
$\nu = 10^{-6}$	0.035	8.142e-01	1.377276	0.24	1.08846	1.376376	10000	2.89	6.089e+01

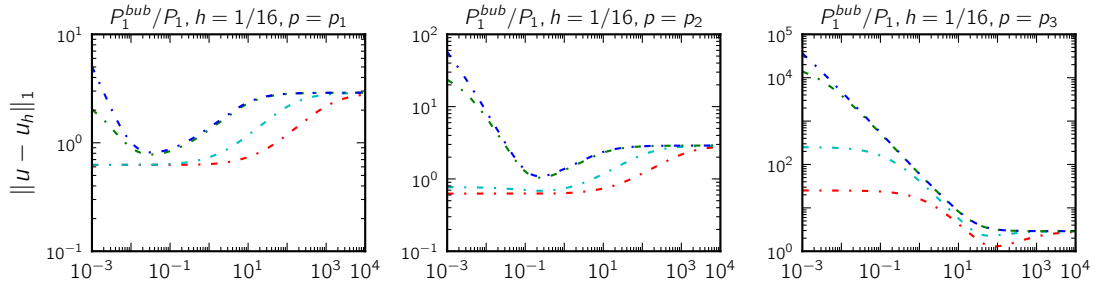

legend	γ	min	$\gamma = 1$, min	γ	min	$\gamma = 1$, min	γ	min	$\gamma = 1$, min
$\nu = 1$	1e-03	3.112e-01	3.158e-01	8e-03	3.113e-01	3.159e-01	44.0	5.407027e-01	3.512006
$\nu = 10^{-1}$	1e-03	3.113e-01	3.594e-01	0.063	3.207e-01	3.599e-01	25.0	1.038956	9.266742
$\nu = 10^{-3}$	0.017	3.686e-01	8.364e-01	0.10	4.840e-01	8.367e-01	25.0	2.299647	1.507e+01
$\nu = 10^{-6}$	0.018	3.959e-01	9.284e-01	0.093	5.364e-01	9.280e-01	27.0	2.37904	1.601e+01

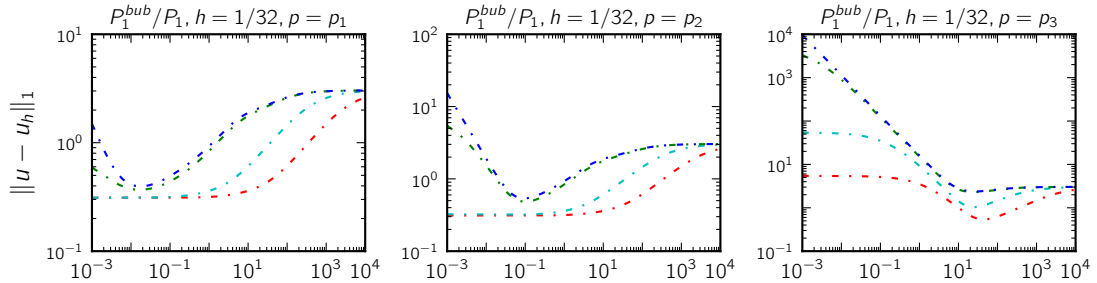

legend	γ	min	$\gamma = 1$, min	γ	min	$\gamma = 1$, min	γ	min	$\gamma = 1$, min
$\nu = 1$	1e-03	1.556e-01	1.580e-01	1e-03	1.556e-01	1.580e-01	30	2.347e-01	9.233e-01
$\nu = 10^{-1}$	1e-03	1.556e-01	1.807e-01	0.017	1.571e-01	1.807e-01	17	4.081e-01	2.463122
$\nu = 10^{-3}$	7e-03	1.798e-01	4.688e-01	0.054	2.362e-01	4.690e-01	97	1.221323	4.411230
$\nu = 10^{-6}$	7e-03	2.072e-01	5.889e-01	0.048	2.911e-01	5.893e-01	10	1.394637	5.018550

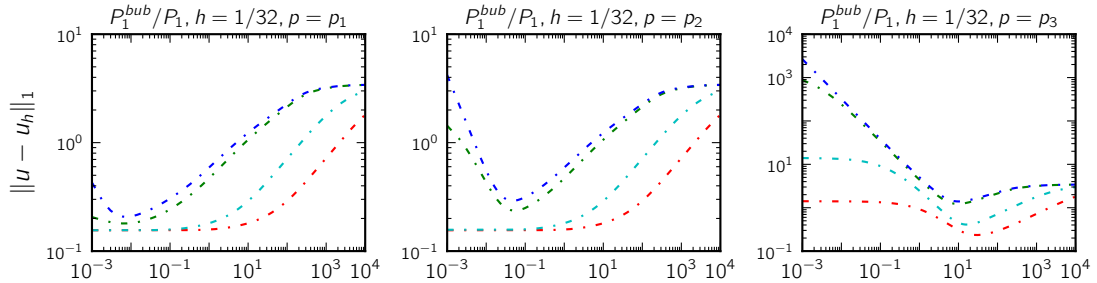

Figure 6: Errors in the H^1-norm of velocity vs. grad-div stabilization parameter γ with $\sigma = 1$ using the MINI element on Delauney-generated triangulations with $h \in \{1/16,\ 1/32,\ 1/64\}$.

4.2. Steady-state flow around a cylinder

The second test problem is considered for the two-dimensional incompressible Navier-Stokes equations. The accuracy of the grad-div stabilization is studied numerically for the benchmark problem of channel flow past a cylinder, introduced in [22]. Figure 7 shows the geometry of the channel with parabolic inflow and outflow is prescribed by

$$\mathbf{u}(0, \mathbf{y}) = \mathbf{u}(2.2, \mathbf{y}) = 0.41^{-2}\big(1.2\mathbf{y}(0.41 - \mathbf{y}), 0\big), \qquad 0 \le \mathbf{y} \le 0.41.$$

In addition, no-slip boundary conditions are enforced along the top and bottom walls. The viscosity is chosen to be $\nu = 10^{-3}$ and the source term $\mathbf{f} = 0$.

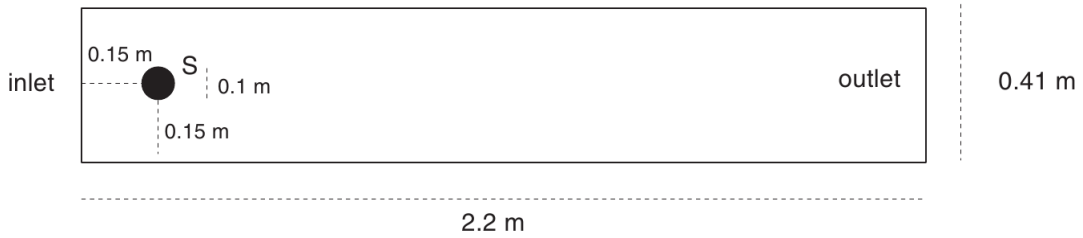

Figure 7: Channel with cylinder

In order to study the accuracy of the grad-div stabilization method, the usual benchmark parameters [14] are the drag coefficient c_d at the cylinder and the lift coefficient c_ℓ defined by, respectively,

$$c_d = -500\big[(\nu\nabla\mathbf{u}, \nabla\mathbf{v}_d) + (\mathbf{u}\cdot\nabla\mathbf{u}, \mathbf{v}_d) - (p, \nabla\cdot\mathbf{v}_d\big]$$
$$c_\ell = -500\big[(\nu\nabla\mathbf{u}, \nabla\mathbf{v}_\ell) + (\mathbf{u}\cdot\nabla\mathbf{u}, \mathbf{v}_\ell) - (p, \nabla\cdot\mathbf{v}_\ell\big]$$

for any function $\mathbf{v}_d \in \big(H^1(\Omega)\big)^2$ with $(\mathbf{v}_d)\big|_S = (1,0)^T$, S being the boundary of the body and $\mathbf{v}_d$ vanishes on all other boundaries. The lift coefficient can be compute in a similar way by using $(\mathbf{v}_\ell)$ as a test function such that $(\mathbf{v}_\ell)\big|_S = (0,1)^T$ on the boundary of the cylinder. A third benchmark parameter is the difference of the pressure between the front and the back of the body

$$\Delta p = p(0.15, 0.2) - p(0.25, 0.2).$$

In the numerical simulations, the standard and Delanay-generated triangulations are used. The initial grids are presented in figure 8, where the standard grid consists of 288 mesh cells and the Delauney grid of 195. The Navier-Stokes equations were discretized by using the inf-sup stable pair of Taylor-Hood $((P_2)^2, P_1)$ and MINI $\big((P_1^{\text{bub}})^2, P_1\big)^2$ finite element. The degrees of freedom for both element on different refinement levels are given in table 1. The accuracy is measured with respect to the distance to the reference values, taken from [14],

$$c_{\text{d,ref}} = 5.57953523384, \quad c_{\text{l,ref}} = 0.010618937712, \quad \Delta p_{\text{ref}} = 0.11752016697.$$

The simulations were performed on different levels of refinements that are presented in Fig. 9 for the $\big((P_2)^2, P_1\big)$ on the standard grids and in Figs. 10 and 11 the $\big((P_1)^{\text{bub}}, P_1\big)$ on the standard and Delauney type grids, respectively. In particular, the errors of the computed values to the reference values are plotted along the varying grad-div stabilization parameter γ. Concerning the accuracy, the best results can be found with the smallest error.

From the numerical simulations, one can see that the optimal γ depends on the quantity of interest, i.e., drag or lift coefficients etc. Fig. 9 for the Taylor-Hood element shows that the optimal γ should be smaller for the drag coefficient compared to the lift coefficient. Moreover, the optimal γ decreases for the lift and increases for the lift coefficient and pressure difference with respect to the mesh width. This shows the dependency of the optimal γ on the mesh width h. One can see in plots of Fig 9 that there are some pronounced peaks with very good results for small values of grad-div parameter which coincides with the best results obtained with higher order finite elements in [14]

On the other hand, for the $\big((P_1)^{\text{bub}}, P_1\big)$ element (see Figs. 10, 11), one can conclude that the grad-div stabilization does not improve the accuracy of the computed solution. Comparing with the reference values one can see that the results are not accurate. In general, numerical simulations shows that the results computed with the Taylor-Hood element are more accurate than with the MINI element. Finally, one can conclude from the experience of these simulations that although the predictions of the corresponding optimal parameters is impossible in practice but the better results can be obtained with small parameters of the grad-div term.

level	$((P_2)^2, P_1)$	$\left((P_1^{\text{bub}})^2, P_1\right)^2$	
	standard	standard	delauney
2	7344	5684	2871
3	28656	2210	11202
4	113184	87776	44244

Table 1: DOF's

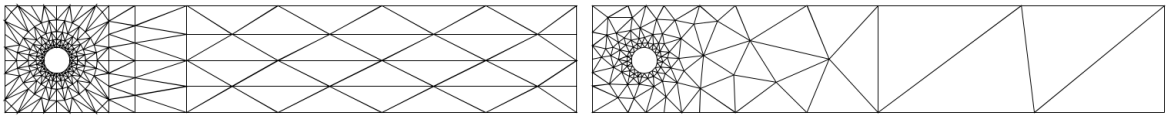

Figure 8: Initial grids: standard left and Delauney right.

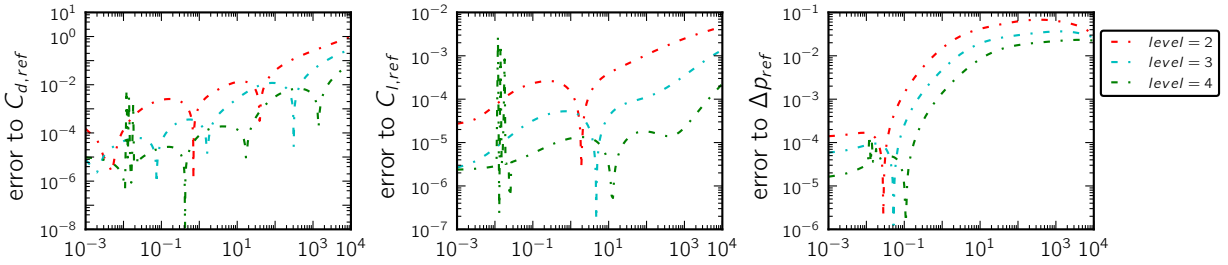

Figure 9: Standard grid with $\left((P_2)^2, P_1\right)$ element: Errors of the computed drag coefficient to $c_{\text{d,ref}}$ (left), lift coefficient to $c_{\text{l,ref}}$ (middle) and pressure difference to Δp_{ref} (right) vs. the grad-stabilization parameter γ on different refinement levels.

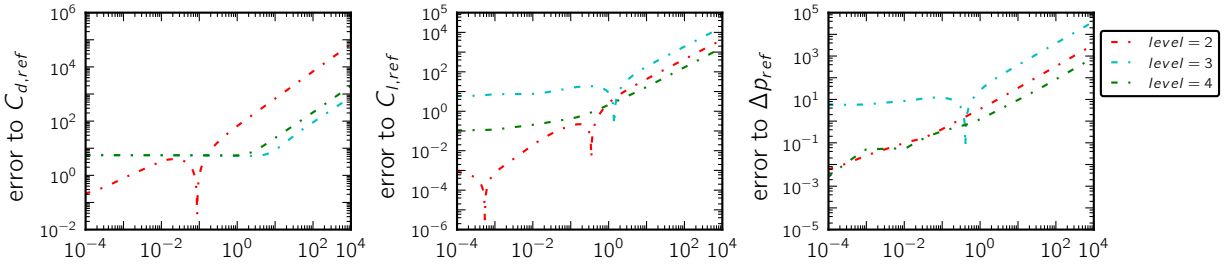

Figure 10: Standard grid with $\left((P_1^{\text{bub}})^2, P_1\right)$ element: Error of the computed drag coefficient to $c_{\text{d,ref}}$ (left), lift coefficient to $c_{\text{l,ref}}$ (middle) and pressure difference to Δp_{ref} (right) vs. the grad-stabilization parameter γ on different refinement levels.

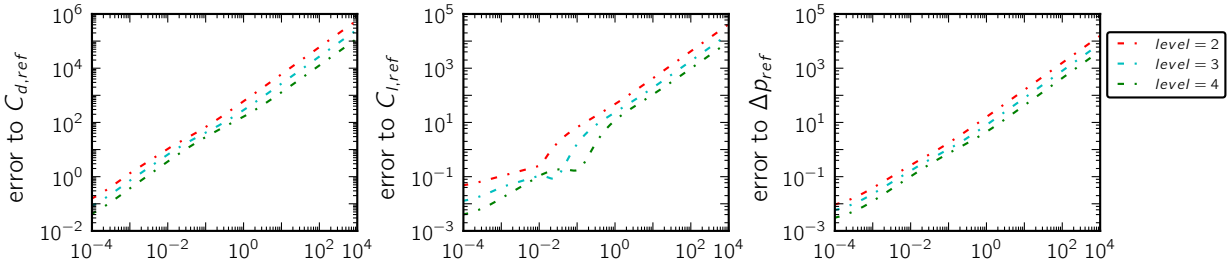

Figure 11: Delauney grid with $\left((P_1^{\text{bub}})^2, P_1\right)$ element: Error of the computed on drag coefficient to $c_{\text{d,ref}}$ (left), lift coefficient to $c_{\text{l,ref}}$ (middle) and pressure difference to Δp_{ref} (right) vs. the grad-stabilization parameter γ on different refinement levels.

5. Summary

This article presented a detailed study of the optimal grad-div stabilization parameter in finite element methods applied to the Oseen and Navier-Stokes equations. The stabilization parameter for the Oseen equations is derived on the basis of minimizing the H^1 error of the velocity. From

the estimates, it was noticed that the optimal parameter choice depends on the used norm , the solution, the finite element spaces, and the type of mesh. It was found that the special case of divergence-free velocity space with optimal approximation properties which leads for the Stokes equations to different grad-div parameters leads to the same parameters for Oseen equations. From a practical point of view, this observation is of advantage since in practice it is hard to decide which case is present. Since there is no difference in the parameter choice, one does not need to care for this issue. Because the reason for obtaining the same optimal parameters is the presence of the convective term in the Oseen equation, it can be expected that for the Navier-Stokes equations the same situation holds like for the Oseen equations.

On the other hand, it was observed both theoretically and numerically that the $H^1(\Omega)$ error of the velocity depends on the inverse of the viscosity parameter. Therefore the error increase by decreasing the viscosity. This observation holds irrespective of the optimal approximation properties of the divergence-free subspace of the velocity space.

With respect to the accuracy of the computed solution, it was shown that the errors computed with the optimal parameter are smaller by several order of magnitudes compared to the errors obtained with parameter of $\mathcal{O}(1)$.

For studying the impact of the grad-div stabilization to the Navier-Stokes equations, numerical studies were performed for a two-dimensional flow around a cylinder. It turns out for the Taylor-Hood element that the smaller values of the grad-div parameter leads to the best results. On the other hand, for the MINI element, accurate results can be obtained without grad-div stabilization.

References

[1] A. N. Brooks, T. J. R. Hughes, Streamline upwind/Petrov-Galerkin formulations for convection dominated flows with particular emphasis on the incompressible Navier-Stokes equations, Comput. Methods Appl. Mech. Engrg. 32 (1-3) (1982) 199–259, fENOMECH '81, Part I (Stuttgart, 1981).

[2] L. P. Franca, S. L. Frey, Stabilized finite element methods. II. The incompressible Navier-Stokes equations, Comput. Methods Appl. Mech. Engrg. 99 (2-3) (1992) 209–233.

[3] P. Hansbo, A. Szepessy, A velocity-pressure streamline diffusion finite element method for the incompressible navier-stokes equation, Comput. Methods Appl. Mech. Eng. 84 (2) (1990) 175–192.

[4] G. Matthies, G. Lube, L. Röhe, Some remarks on residual-based stabilisation of inf-sup stable discretisations of the generalised Oseen problem, Comput. Methods Appl. Math. 9 (4) (2009) 368–390.

[5] Y. Bazilevs, V. M. Calo, J. A. Cottrell, T. J. R. Hughes, A. Reali, G. Scovazzi, Variational multiscale residual-based turbulence modeling for large eddy simulation of incompressible flows, Comput. Methods Appl. Mech. Engrg. 197 (1-4) (2007) 173–201.

[6] T. J. R. Hughes, G. R. Feijóo, L. Mazzei, J.-B. Quincy, The variational multiscale method—a paradigm for computational mechanics, Comput. Methods Appl. Mech. Engrg. 166 (1-2) (1998) 3–24.

[7] V. John, A. Kindl, Numerical studies of finite element variational multiscale methods for turbulent flow simulations, Comput. Methods Appl. Mech. Engrg. 199 (13-16) (2010) 841–852.

[8] M. Olshanskii, G. Lube, T. Heister, J. Löwe, Grad-div stabilization and subgrid pressure models for the incompressible Navier-Stokes equations, Comput. Methods Appl. Mech. Engrg. 198 (49-52) (2009) 3975–3988.

[9] M. A. Olshanskii, A low order Galerkin finite element method for the Navier-Stokes equations of steady incompressible flow: a stabilization issue and iterative methods, Comput. Methods Appl. Mech. Engrg. 191 (47-48) (2002) 5515–5536.

[10] H.-G. Roos, M. Stynes, L. Tobiska, Robust numerical methods for singularly perturbed differential equations, 2nd Edition, Vol. 24 of Springer Series in Computational Mathematics, Springer-Verlag, Berlin, 2008.

[11] M. Braack, E. Burman, V. John, G. Lube, Stabilized finite element methods for the generalized Oseen problem, Comput. Methods Appl. Mech. Engrg. 196 (4-6) (2007) 853–866.

[12] K. J. Galvin, A. Linke, L. G. Rebholz, N. E. Wilson, Stabilizing poor mass conservation in incompressible flow problems with large irrotational forcing and application to thermal convection, Comput. Methods Appl. Mech. Engrg. 237/240 (2012) 166–176.

[13] E. W. Jenkins, V. John, A. Linke, L. G. Rebholz, On the parameter choice in grad-div stabilization for the Stokes equations, Adv. Comput. Math. 40 (2) (2014) 491–516.

[14] V. John, G. Matthies, Higher-order finite element discretizations in a benchmark problem for incompressible flows, International Journal for Numerical Methods in Fluids 37 (8) (2001) 885–903.

[15] L. P. Franca, S. L. Frey, Stabilized finite element methods. II. The incompressible Navier-Stokes equations, Comput. Methods Appl. Mech. Engrg. 99 (2-3) (1992) 209–233.

[16] T. J. R. Hughes, L. P. Franca, M. Balestra, A new finite element formulation for computational fluid dynamics. V. Circumventing the Babu**v**ska-Brezzi condition: a stable Petrov-Galerkin formulation of the Stokes problem accommodating equal-order interpolations, Comput. Methods Appl. Mech. Engrg. 59 (1) (1986) 85–99.

[17] R. Pierre, Simple C^0 approximations for the computation of incompressible flows, Comput. Methods Appl. Mech. Engrg. 68 (2) (1988) 205–227.

[18] V. John, G. Matthies, MooNMD—a program package based on mapped finite element methods, Comput. Vis. Sci. 6 (2-3) (2004) 163–169.

[19] D. N. Arnold, F. Brezzi, M. Fortin, A stable finite element for the Stokes equations, Calcolo 21 (4) (1984) 337–344 (1985).

[20] D. N. Arnold, Q. Jinshui, Quadratic velocity/linear pressure stokes elements, in: Advances in Computer Methods for Partial Differential Equations VII, IMACS, 1992, pp. 28–34.

[21] S. Zhang, Bases for $C0-P1$ divergence-free elements and for $C1-P2$ finite elements on union jack grid, 2012, Submitted.

[22] S. Turek, M. Schäfer, Benchmark computations of laminar flow around cylinder, in: E. Hirschel (Ed.), Flow Simulation with High-Performance Computers II, Vol. 52, Vieweg, 1996, pp. 547–566.